2

UCRL-CR-116829
S/C - B235292

ER-20037 LLNL Eternal Pathfinder Wing Spar Design Study Report

EDO Corporation, Fiber Science Division

March 1994

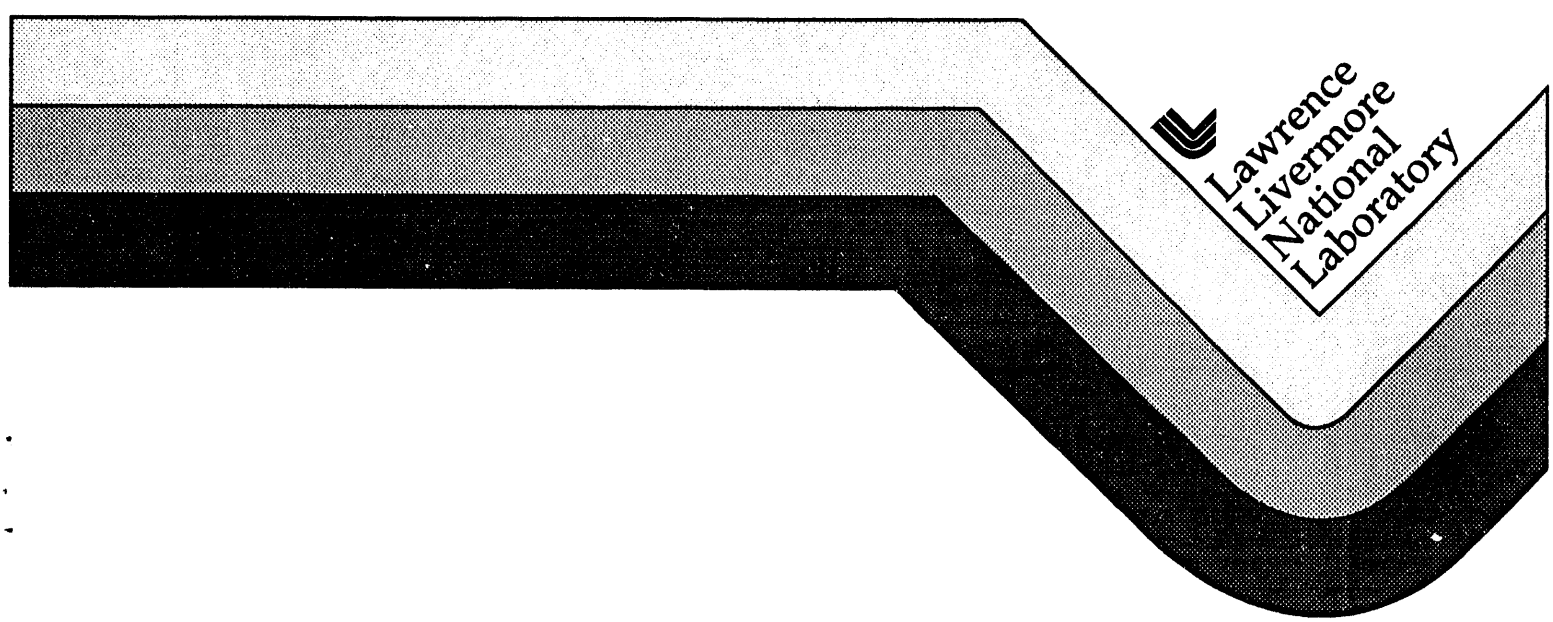

DISCLAIMER

REVISION HISTORY			
LTR	DESCRIPTION	DATE	APPD
N/C	Original Release per ECN A5475	12 Jul 93	DM

REV. STATUS
OF SHEETS: ALL SHEETS -

DRAWN	-	-
CHECK	-	-
STRESS	-	-
WEIGHT	-	-
Q.C.		
MFG.ENGR.		
PROJ.ENGR.	D.J.Moser	DJMoser
PROG.MGR.	R.Cockrell	
APPROVAL	-	-
APPROVAL	-	-
RELEASE DATE:	12 Jul 93	

EDO CORPORATION - FIBER SCIENCE DIVISION
SALT LAKE CITY, UTAH 84116

TITLE:
LLNL
ETERNAL PATHFINDER WING SPAR
DESIGN STUDY REPORT

SIZE	CODE IDENT	DWG. NO.	REV.
A	32500	ER-20037	-

SCALE:	UNIT WT:	SHEET
N/A	N/A	1 of 12

ER-20037

LLNL

ETERNAL PATHFINDER WING SPAR

DESIGN STUDY REPORT

TABLE OF CONTENTS

LIST OF TABLES

LIST OF APPENDICES

1.0 INTRODUCTION

This document outlines the results of a design study performed by EDO-FSD on the LLNL Eternal Pathfinder Wing Spar/Fuel Tank. The main focus of the design study was the weight minimization of the composite wall of the mid span spar section of the aircraft. The torque, shear, moment and pressure loading requirements, as well as LLNL's preliminary drawings, were used to develop a reduced weight mid-span spar design. The design study also encompassed details such as the pressure bulkheads, wing rod connectors, and attachment flanges.

2.0 APPLICABLE DOCUMENTS

2.1 LLNL Statement of Work, with Attachments A, B, and C.

2.2 EDO-FSD Technical Proposal, SQ 2294

2.3 EDO-FSD Drawing 3728-001

3.0 DESIGN REQUIREMENTS SUMMARY

(See Appendix A for more detailed information)

3.1 The spar is to contain 300 psi oxygen and hydrogen gases in separate compartments. It was also assumed that a 300 psi differential pressure between the hydrogen and oxygen compartments could occur. The spar is required to react the pressure-induced stresses only, and is not expected to provide a leak-proof barrier to the pressurized gases.

3.2 The entire length of the spar is to react a worst case 9,800 in-lb torsion load during a +1 g maximum control surface deflection.

3.3 At the worst case of +5 g flight load, the inboard portion of the spar is to react a maximum force of 349,000 in-lb bending moment about the roll axis of the aircraft. The outboard portion of the spar experiences a maximum bending moment of 206,000 in-lb, with areas in between varying linearly wight spanwise position.

3.4 The factor of safety is 2.0 for all internal pressure, torsion, moment and shear loads on the main body of the spar. The spar fittings are to have a safety factor of 3.0.

3.5 The eight possible loading case combinations are as follows:

3.5.1 +5 g flight load with internal pressure
3.5.2 -3 g flight load with internal pressure
3.5.3 Full control surface deflection with internal pressure
3.5.4 Hard landing loads with internal pressure
3.5.5 +5 g flight load without internal pressure
3.5.6 -3 g flight load without internal pressure
3.5.7 Full control surface deflection without internal pressure
3.5.8 Hard landing loads without internal pressure

4.0 BASELINE DESIGN AND WEIGHT REDUCTION CONSIDERATIONS

4.1 As a point-of-departure design (see Appendix B for more detailed information), the baseline spar design has the following features:

4.1.1 Filament-wound carbon fiber/epoxy plies (90°, ±10°, and ±45°)
4.1.2 Honeycomb core sandwich with localized reinforcements
4.1.3 Uni-directional carbon fiber/epoxy spar caps plies (0°)
4.1.4 Machined Aluminum bulkheads and flanges, bolted attachments
4.1.5 Filament-wound carbon fiber/epoxy wing rods with stiffening rings

4.2 Since the mid-span spar section is subjected to varying bending moments (see 3.3 above), the spar cap plies can be tailored to enable further weight reductions. However, the other plies were required along the entire length of the spar to react the shear, torsion, and internal pressure loading conditions. Areas where stresses are highly localized, such as machined holes and loading surfaces, can be reinforced with woven plies of carbon fiber/epoxy composite and/or an epoxy resin/glass microballoons foam filler.

4.3 The most challenging loading conditions were found to be the +5 g load, with and without internal pressure. In the unpressurized condition, the compressive stress induced by the bending moment has the potential for a localized buckling failure mode. A lightweight and effective technique for dealing with this threat of buckling is the addition of a core material, such as aramid honeycomb, between the spar cap longos. The following formula (from "Roark's Formulas ... " by Young, table 35, case 16) was used to estimate the critical bending moment for localized buckling on a thin wall tube.

$$M_{crit} = \frac{K * E * r * t^2}{[1 - \gamma_2]}$$

In this calculation, it was assumed that $E=E_{axial}$ and that $K/[1-\gamma^2]=1$. This formula accentuates the high sensitivity of wall thickness. Using the laminate data based on high strength/ moderate stiffness fiber, it was determined that the safety factor for localized buckling is 3.40. It is not known if this localized buckling will result in actual fiber failure, or merely excessive spar deflection. It should be noted that this formula is for a solid wall tube with isotropic material properties, when in fact the tube wall is a sandwich construction with anisotropic material properties. Using empirically derived data on similar structures is the only reliable means of predicting failure. Unfortunately, no such data was available for this study.

4.4 Fiber grade selection was based on a strength vs. stiffness trade-offs. As mentioned above the addition of honeycomb core was very effective in reducing elastic stability problems, more effective than the option of high modulus, moderate strength carbon fiber. The high tensile stresses that result from combined internal pressure and bending moment make high strength fibers more desirable than high modulus fibers, especially since the buckling safety factor is predicted to be adequate with the moderate modulus fibers. If it turns out that buckling occurs at a lower bending moment than predicted, or if less wing deflection is desired, then the addition of high modulus fibers in the spar caps will be warranted.

T-700S fiber, claimed by Toray to have a 711 ksi tensile strength, was selected as the baseline fiber throughout the spar. It's tensile modulus is 33.4 Msi. Cost is currently $15/lb.

T-1000G fiber is a premium grade high strength fiber with a reported tensile strength of 924 ksi, a 30% improvement over T-700S. It's tensile modulus is 42.7 Msi, 28% higher than T-700S. It is, however, quite expensive at $75/lb, and not always readily available. Also, switching fiber grades will not always result in weight reductions. For example, reducing the helical ply thicknesses to take advantage of the higher strength fibers also reduces the spar's axial stiffness, resulting in a lower critical buckling stress. T-1000G fiber may be useful in the hoop layer where strength can be enhanced without sacrificing the spar's axial stiffness.

4.5 The manufacturing process considerations, outlined in Appendix C, were very influential in determining certain features in the design. The two main tooling options for fabricating the main body of the spar are (1) a solid Aluminum mandrel, 0.5 inch thick, and (2) a hybrid inflatable mandrel with metal locating features and a fiber reinforced rubber skin whose rigidity is controlled by internal pressure. The Aluminum mandrel can be machined to fairly tight tolerances, but it will be expensive to build and will sag approximately 0.9 inch when supported on the ends. The thermal expansion of the Aluminum will compact the spar laminate, but may induce fiber strains of up to 0.5%. It also may be quite difficult to extract the mandrel from the cured spar. The hybrid inflatable is less expensive, easy to extract, and can control laminate compaction pressure directly. Once it is pressurized, there should be negligible sag with the hybrid inflatable mandrel, but it may be difficult to achieve a diameter tolerance ± 0.030 inch or less.

4.6 Since a minimum weight spar is the primary objective of this design study, it was necessary to determine which specific components of the spar could be safely lightened while still maintaining its overall load bearing capability. Table 4.6-1 summarizes these separate component weights for the baseline design, and a reduced weight option, as described in section 7.2.

TABLE 4.6-1: SPAR WEIGHT SUMMARY		
Component	**Baseline Design**	**Improved Design**
± 45° helical	15.1	7.6
0° spar caps	10.5	6.3
± 10° helical	12.6	10.1
90° hoop[1]	12.6	11.3
Honeycomb core	8.0	4.8
Foam filler	1.5	1.0
Cloth reinforcements	0.4	0.4
Wing rod	10.5	8.0
Bulkheads & Flanges	4.1	4.1
TOTAL	75.7 pounds	53.6 pounds

5.0 LAMINATE PROPERTY ANALYSIS RESULTS

(See Appendix D)

5.1 The computer program "ABD1" was used to predict the macroscopic stiffness and strength properties of the proposed sandwich laminate. This program is based on classical lamination theory, which considers the in-plane elastic response of multiple anisotropic material layers at various angular orientations.

5.2 ABD1 also utilizes a proven data base of AS-4/3501-6 failure properties to predict the tensile and compressive loads at which a laminate is likely to fail. Since the higher strength T-700 carbon fiber was baselined in the spar design, the fiber stress load ratios can be scaled up accordingly, *but only for laminate plies in tension.* Compressive failure properties are far less predictable than tensile, and much debate still surrounds theories and test methods for composite compressive failure. Ultimate compressive strength is affected by factors such as the resin shear modulus, laminate void content, fiber volume, and fiber straightness. Since compressive strength is so sensitive to processing and structure-specific characteristics, test data is much preferred over analytical predictions.

---

[1] *The mass of the hoop layer alone is necessary and sufficient to react the internal pressure loading. The mass of the other plies must be present with or without internal pressure. Upgrading to T-100G fiber in the hoop ply only would reduce the spar's weight by another 2.9 pounds.*

5.3 The *Tsai-Wu* failure criterion is useful in predicting the onset of resin matrix cracking, or "first ply failure". However, Tsai-Wu is less capable than either the *fiber stress* or *fiber strain* criterion in the prediction of the laminate's ultimate load bearing capabilities. All three failure criteria are calculated by ABD1 to predict the load ratio at both the top and bottom surfaces of each ply.

5.4 The baseline laminate was input into ABD1 as a symmetrical laminate, even though the actual laminate is asymmetrical. This was done because a symmetrical laminate simulates the actual situation of a near zero curvature change constraint (**K** vector=0), which the program cannot directly control. Since no moment loads were applied, and **B** matrix=0, due to the laminate's symmetry, the value of the **D** matrix was unimportant. The **A** matrix and load ratio data were the only meaningful results from this analysis.

5.5 The load ratios, or safety factors, for each material layer at the two most severe loading conditions are given in Table 5.5-1. In this analysis, the loads applied to the laminate represented an evenly distributed load over the entire width of the spar cap region. The "*fstress*" and "TW" designations represent the load ratios from the fiber stress and Tsai-Wu failure criteria predictions. Note that even though first ply failure is predicted in the fully pressurized condition, the factor of safety still exceeds the minimum of 2. Also note that the *fstress* load ration for the 0° and ±10° plies increases slightly when the spar becomes pressurized.

TABLE 5.6-1: ABD1 RESULTS

Ply	Bending Moment Compression Side	Moment and Pressure Tension Side
90°	fstress=49.0, TW=10.3	*fstress=3.9, TW=1.1
±10°	fstress=5.3, TW=5.1	*fstress=7.4, TW=0.8
0°	fstress=5.2, TW=5.5	*fstress=7.7, TW=0.8
±45°	fstress=12.6, TW=4.2	*fstress=5.2, TW=0.9

** Load ratios increased by 40% to account for the higher fiber strength of T-700*

E_{axial} = 2.134 Msi
E_{trans} = 1.084 Msi
$G_{in\text{-}plane}$ = 0.314 Msi

6.0 FINITE ELEMENT ANALYSIS RESULTS

(see Appendix E)

6.1 A sample section of the spar was analyzed with COSMOS/M finite element analysis software. This analysis technique is helpful in illustrating stress distributions and deflections in an arbitrary structural shape. A 60 inch long section of the spar was modeled using 4-node quadrilateral layered composite shell elements. The model was subjected to the maximum torsion, bending moment, and internal pressure loading conditions as specified in Appendix A. Combined pressure and moment loading was also considered.

6.2 The 2,000 element model was constrained by specifying zero angular and axial displacement at all nodes at one end of the tube. One of the nodes at this end was also radially constrained at zero displacement in order to avoid a singular matrix error in the mathematical solution. The torsion, pressure, and bending moment loads were then applied at the opposite tube end. The material properties, thicknesses, and ply orientations were also entered prior to running the linear static solution. The stress results were calculated in material coordinates so that the values could more easily be related to the fiber stress failure criterion.

6.3 The maximum indicated laminate stress in the 9,800 in-lb torsional loading condition was 7,980 psi in the ± 10° helical layer. However, this maxima was highly localized near the zero radial constraint node, and is therefore probably not a real phenomena. The majority of the spar is stressed at 4,900 to 7,000 psi. These stresses are very low, raising the possibility of ±45° helical layer thickness reduction.

6.4 Under 300 psi internal pressure loading, a maximum stress of 150,000 psi was indicated in the hoop layer with most of the hoop layer stresses above 100,000 psi. The ±10° helical layer was stressed at 18,000 to 41,000 psi, experiencing lower stresses in the areas where the 0° plies were able to react the loads. The ±45° helical layers were stressed up to 73,600 psi. It should be noted that if the

±45° helical layer is to be reduced, the other layers will be somewhat more highly stressed than indicated here.

6.5 When subjected to a bending moment of 350,000 in-lb alone, a maximum stress of ±46,400 psi occurred in the 0° plies. The maximum stress in the ±10° helical layer was ±27,800 psi. The ±45° helical layers were only stressed to a maximum of ±20,020 psi, which is still 3 times the stress level obtained at maximum torsion. The spar's maximum deflection at the free end was 0.787 inch with little indicated tendency for the spar to become oblong.

6.6 In order to properly analyze the combined loading of 300 psi internal pressure and 350,000 in-lb bending moment, it was necessary to include the in-plane stress effects into the solution. The maximum total deflection under this combined loading condition was reduced to 0.599 inch, most of that in the vertical direction. The axial deflection at the loaded end ranged from -0.0236 inch to 0.156 inch. The maximum stresses in the 0° plies were -26,800 and 71,100 psi. In the ±10° helical layer, the maximum stresses were -9,030 and 51,500 psi. The ±45° helical layers were stressed from 20,090 to 84,700 psi, their most severe stress state yet.

7.0 RECOMMENDATIONS FOR DESIGN OPTIMIZATION

7.1 Build and test a baseline spar section to verify the analytical predictions outlined above. The ultimate bending moment would be the most important test data at this stage of the program. The results of this test are essential in order to successfully guide the spar design in the direction of minimum weight. Once the reduced-weight design features have been identified, other sub-scale articles should be built and tested to verify the design's integrity.

7.2 Recommended weight reduction measures:

7.2.1 Reduce thickness of the ±45° helical plies by 50%, 0° and ±10° plies by 20%, and the 90° hoop ply by 10%.

7.2.2 Utilize 1.8 lb/cu. ft. honeycomb instead of 3.0 lb/cu. ft.

7.2.3 Use less resin in the resin/glass microballoons mixture.

7.3 Research alternative joint configurations. It might be possible to not only reduce the spar weight, but also eliminate the wing rod connection detail, thereby allowing a larger usable gas storage volume.

7.4 Research the use of composite materials in bulkheads, flanges and other hardware details. Some weight savings may be realized by switching from machined Aluminum to molded carbon cloth reinforced epoxy parts.

7.5 Maintain a manufacturability and serviceability perspective when specifying dimensional tolerances, part configurations, and materials. An optimum design is of little use if the part cannot be built or operated efficiently.

APPENDIX A

SPAR DESIGN REQUIREMENTS

LEFT MID SEMI-SPAN SPAR CONTROL +5g FLIGHT
MOMENT (ft lb)

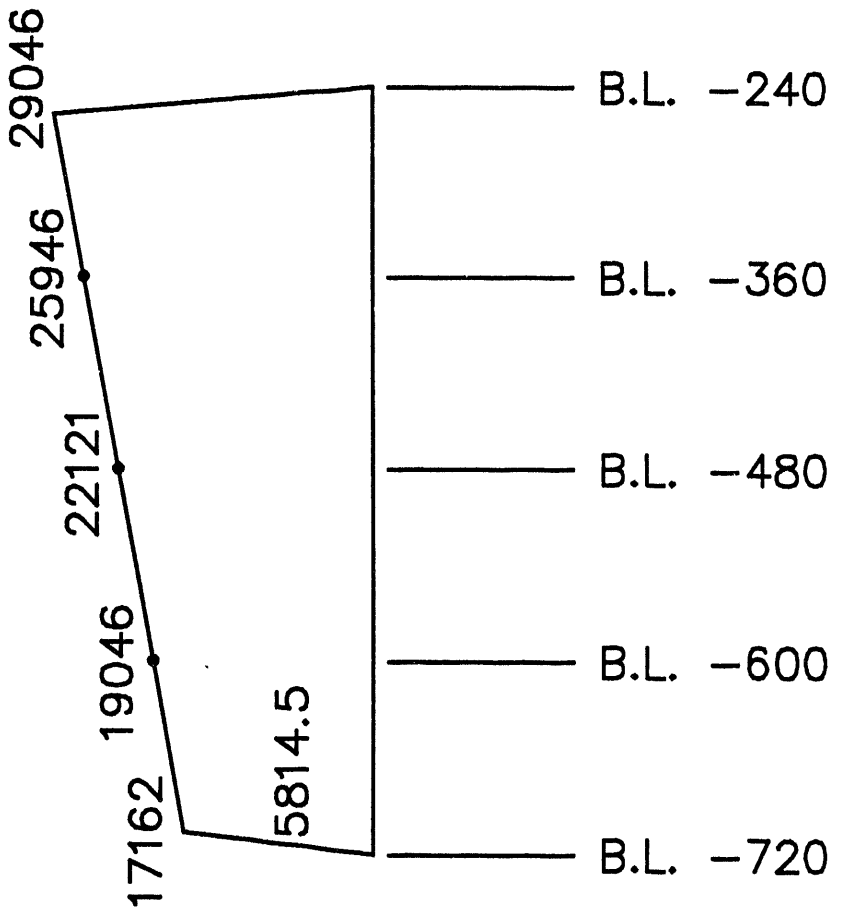

LEFT MID SEMI-SPAN SPAR CONTROL DEFECTION TORSION (ft/lb)
(RIGHT HAND TWIST IS POSITIVE)

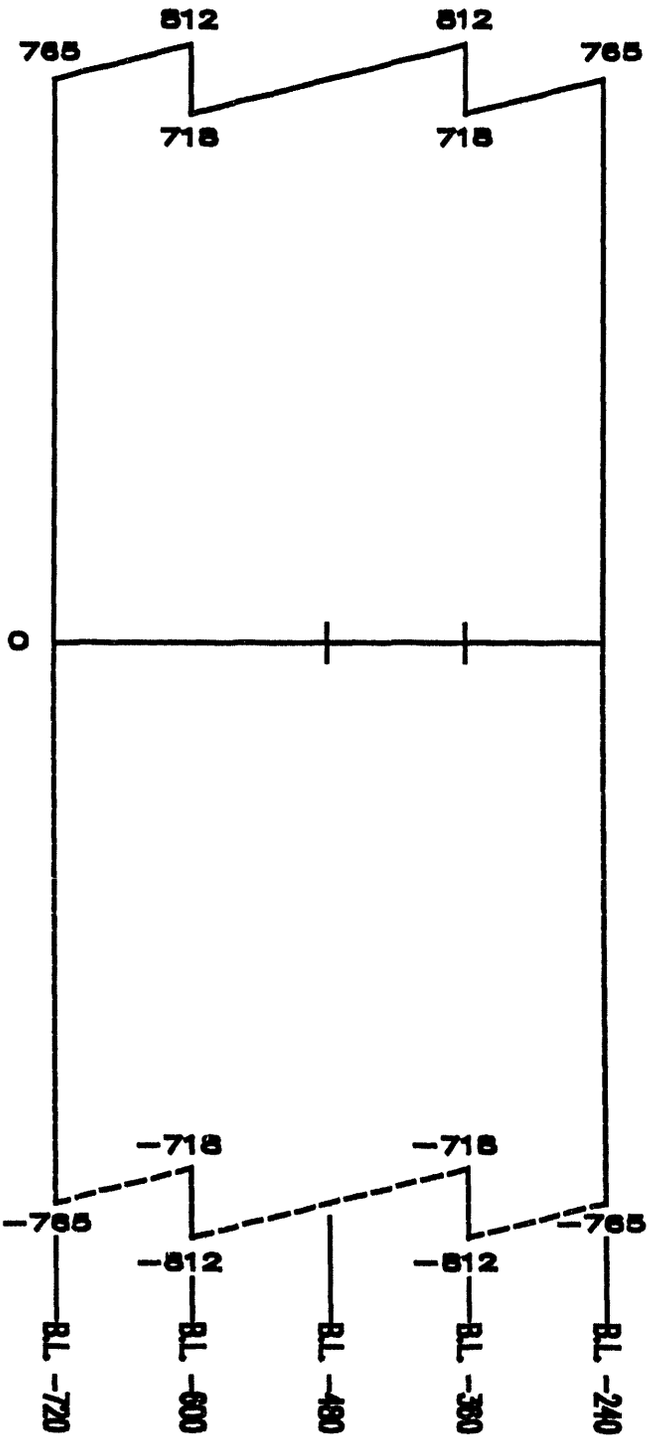

w:\wp-files

EDO CORPORATION FIBER SCIENCE DIVISION

NO. ER-20037 APPENDIX A

DATE: 12 July 1993 PAGE 3 OF 3

995J0024

APPENDIX B

BASELINE SPAR DESIGN

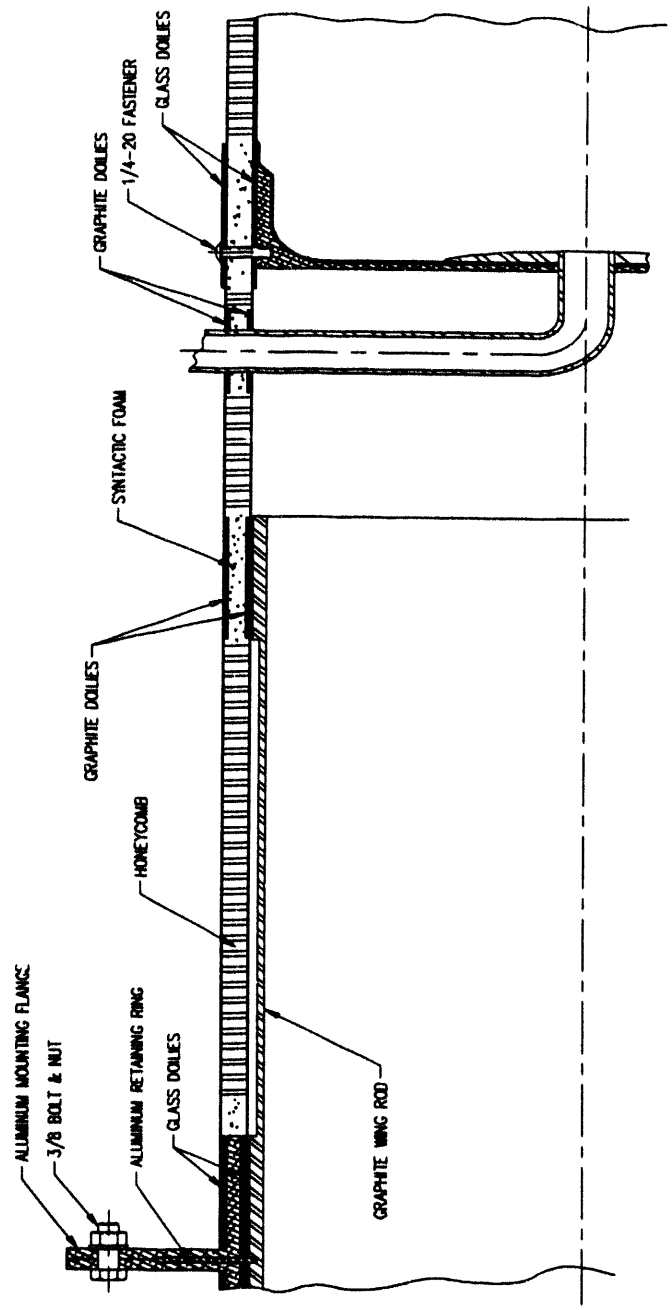
GLASS DOILIES
1/4-20 FASTENER
GRAPHITE DOILIES
SYNTACTIC FOAM
GRAPHITE DOILIES
HONEYCOMB
ALUMINUM MOUNTING FLANGE
3/8 BOLT & NUT
ALUMINUM RETAINING RING
GLASS DOILIES
GRAPHITE WING ROD

APPENDIX C

SPAR MANUFACTURING PROCESS

LLNL
WING SPAR
WINDING / SUBASSEMBLY

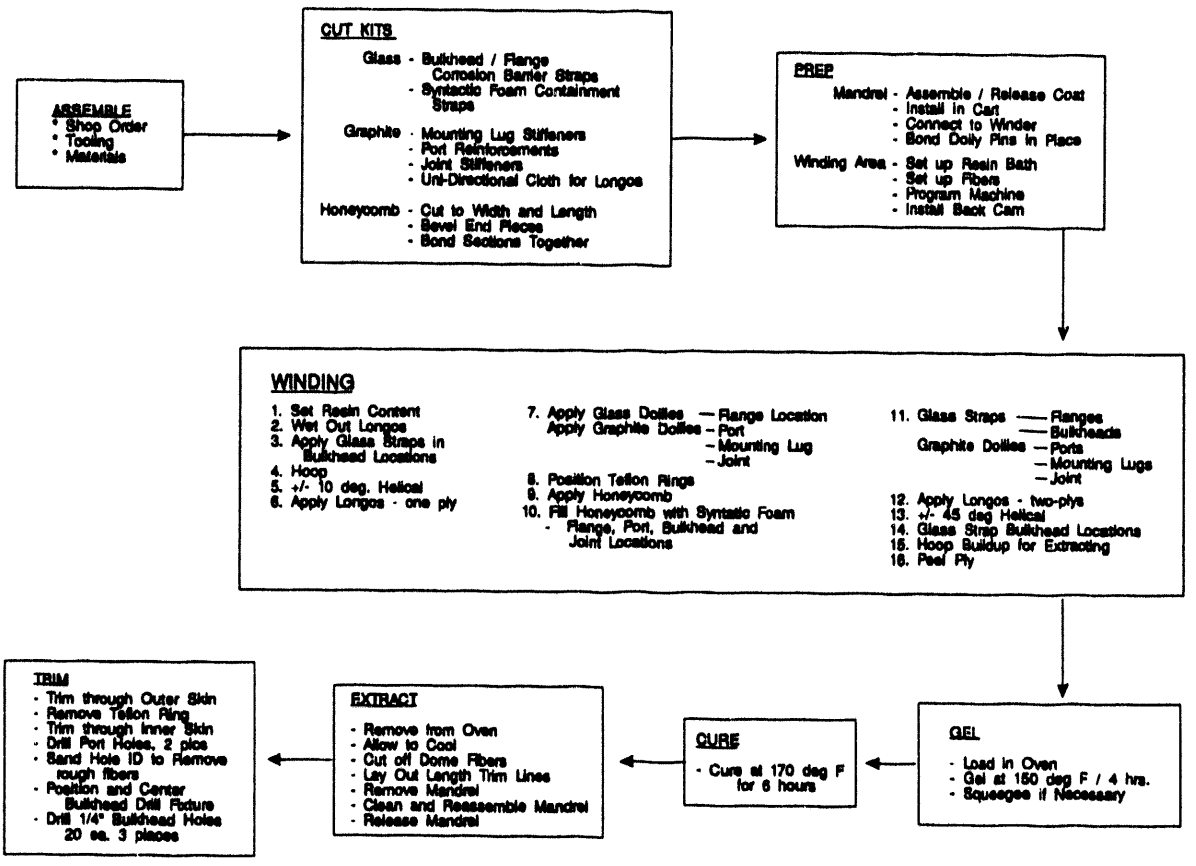

LLNL
WING ROD
FABRICATION

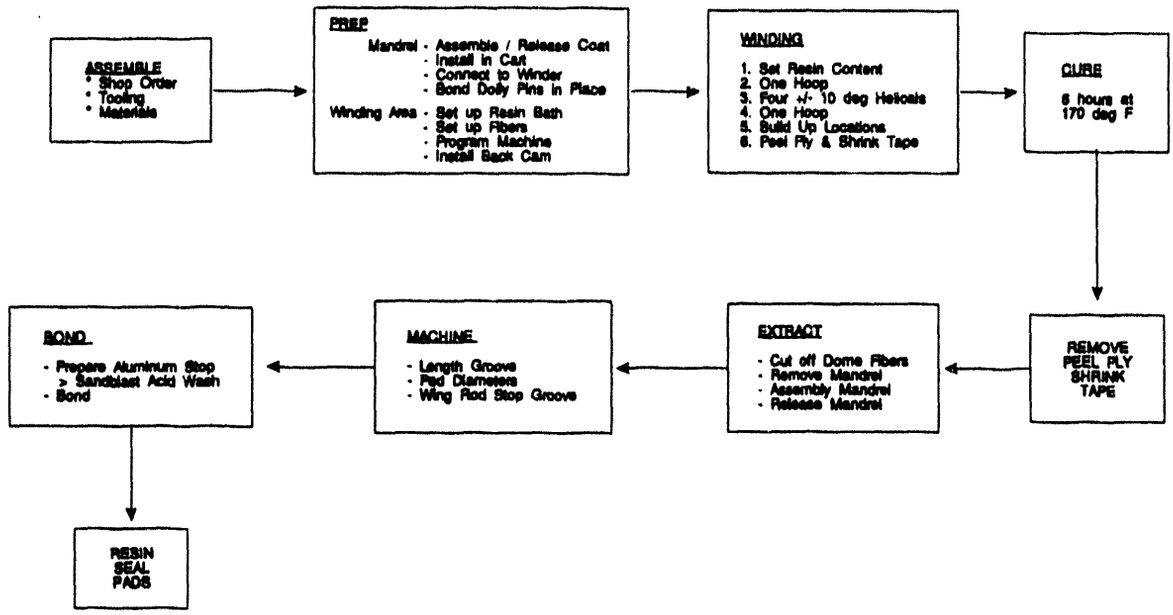

LLNL
WING SPAR
ASSEMBLY

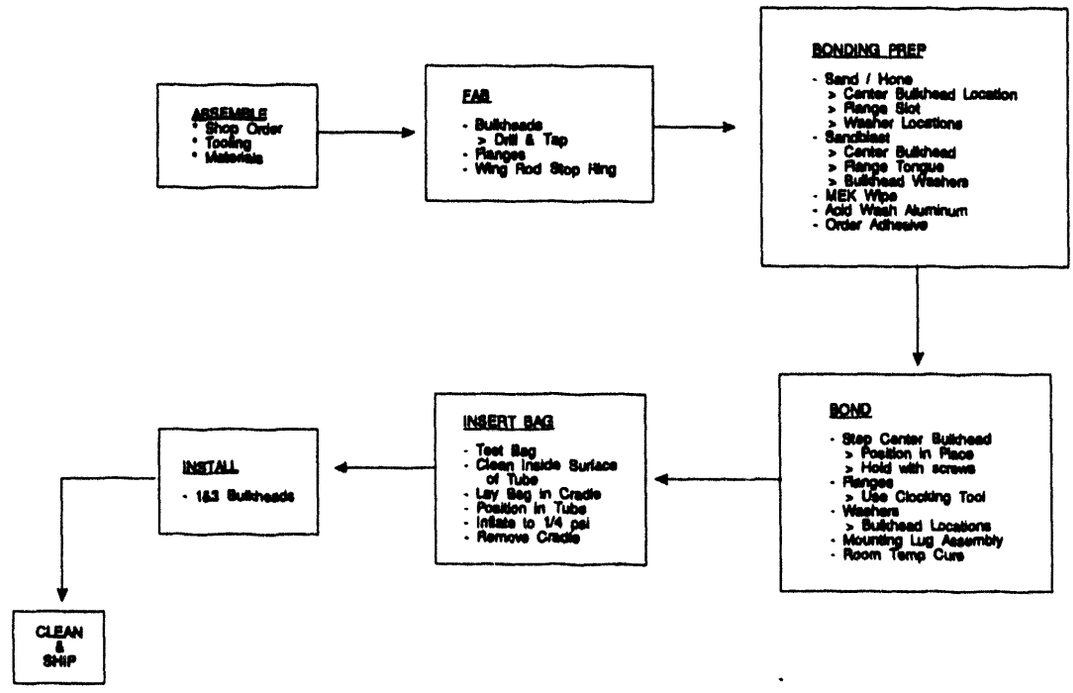

APPENDIX D

LAMINATE ANALYSIS

Laminate Analysis

Moduli for carbon/epoxy (material 1)

E11 =	1.840000E+07	E22=	1600000.000000
Nu12=	2.800000E-01	G=	950000.000000
alpha(1)=	-3.500000E-08	alpha(2)=	1.600000E-05

Moduli for core (material 3)

E11=	10.000000	E22=	10.000000
Nu12=	3.000000E-01	G=	7.000000
alpha(1)=	5.000000E-05	alpha(2)=	5.000000E-05

the input ply groups follow

ply group	Thickness (in)	angle material
1 thickness	2.500000E-03	-45 carbon
2 thickness	2.500000E-03	45 carbon
3 thickness	1.000000E-02	0 carbon
4 thickness	3.000000E-03	10 carbon
5 thickness	3.000000E-03	-10 carbon
6 thickness	6.000000E-03	90 carbon
7 thickness	1.250000E-01	0 core
8 thickness	1.250000E-01	0 core
9 thickness	6.000000E-03	90 carbon
10 thickness	3.000000E-03	-10 carbon
11 thickness	3.000000E-03	10 carbon
12 thickness	1.000000E-02	0 carbon
13 thickness	2.500000E-03	45 carbon
14 thickness	2.500000E-03	45 carbon

The total laminate thickness = 3.040000E-01

A/thickness ($\bar{Q}$) matrix

2180058.000000	224879.700000	-1.038115E-03
224879.700000	1107475.000000	2.868135E-03
-1.243707E-03	2.662543E-03	313507.500000

A MATRIX

662737.400000	68363.420000	7.050543E-04
68363.420000	336672.400000	7.050543E-04
-5.449457E-04	-5.449457E-04	95306.290000

B MATRIX

-8.118089E-02	-1.405256E-03	9.945170E-03
-1.405256E-03	4.381911E-02	7.898966E-04
1.000087E-02	7.235296E-04	-2.158222E-03

D MATRIX

12964.590000	1428.532000	-2.846535
1428.532000	6040.919000	-14.810940
-2.846503	-14.810920	1946.980000

inverse of A/thickness ($\bar{Q}$ inverse) matrix

4.685170E-07	-9.513531E-08	2.421745E-15
-9.513531E-08	9.222728E-07	-8.752468E-15
2.666602E-15	-8.210047E-15	3.189716E-06

Ex= 2134394.000000
Ey= 1084278.000000
Gxy= 313507.500000

A INVERSE MATRIX

1.541175E-06	-3.129451E-07	-9.086162E-15
-3.129450E-07	3.033792E-06	-2.012820E-14
7.022815E-15	1.555735E-14	1.049249E-05

D INVERSE MATRIX

7.919681E-05	-1.872820E-05	-2.668013E-08
-1.872820E-05	1.699696E-04	1.265600E-06
-2.668128E-08	1.265599E-06	5.136255E-04

Failure properties of carbon/epoxy (material 1)

Xt= 257,600 Xc= -151,000
Yt= 6,950 Yc= 24,400 S= 13,880
fiber strain in tension = 1.400000E-02
fiber strain in comp. = -8.200000E-03

Failure properties of core (material 3)

Xt= 10 Xc= -10
Yt= 10 Yc= -10 S=7
fiber strain in tension = 1.000000
fiber strain in comp. = 1.000000

The ratio of failure load to input load is calculated for each surface (top and bottom) of each ply group
Applied stress resultants Nx, Ny, Nxy are:

-1031.000000	0.000000E+00	0.000000E+00

Applied moment resultants Mx, My, Mxy are:

0-000000E+00	0.000000E+00	0.000000E+00

Note: load ratio is the predicted multiple of input loads at failure.

APPENDIX E

FINITE ELEMENT ANALYSIS

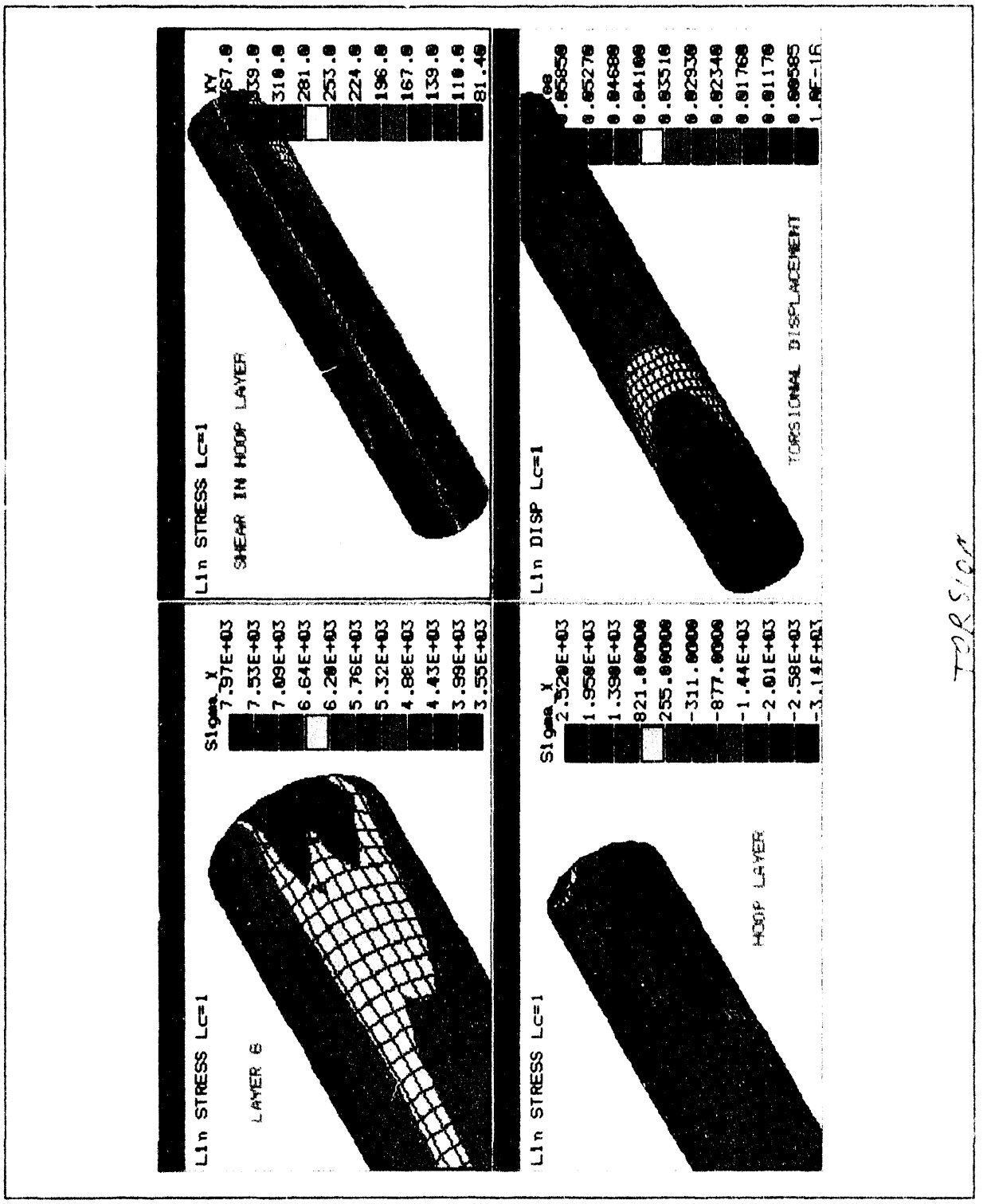
Lin STRESS Lc=1
SHEAR IN HOOP LAYER
Lin DISP Lc=1
TORSIONAL DISPLACEMENT
Lin STRESS Lc=1
LAYER 6
Lin STRESS Lc=1
HOOP LAYER

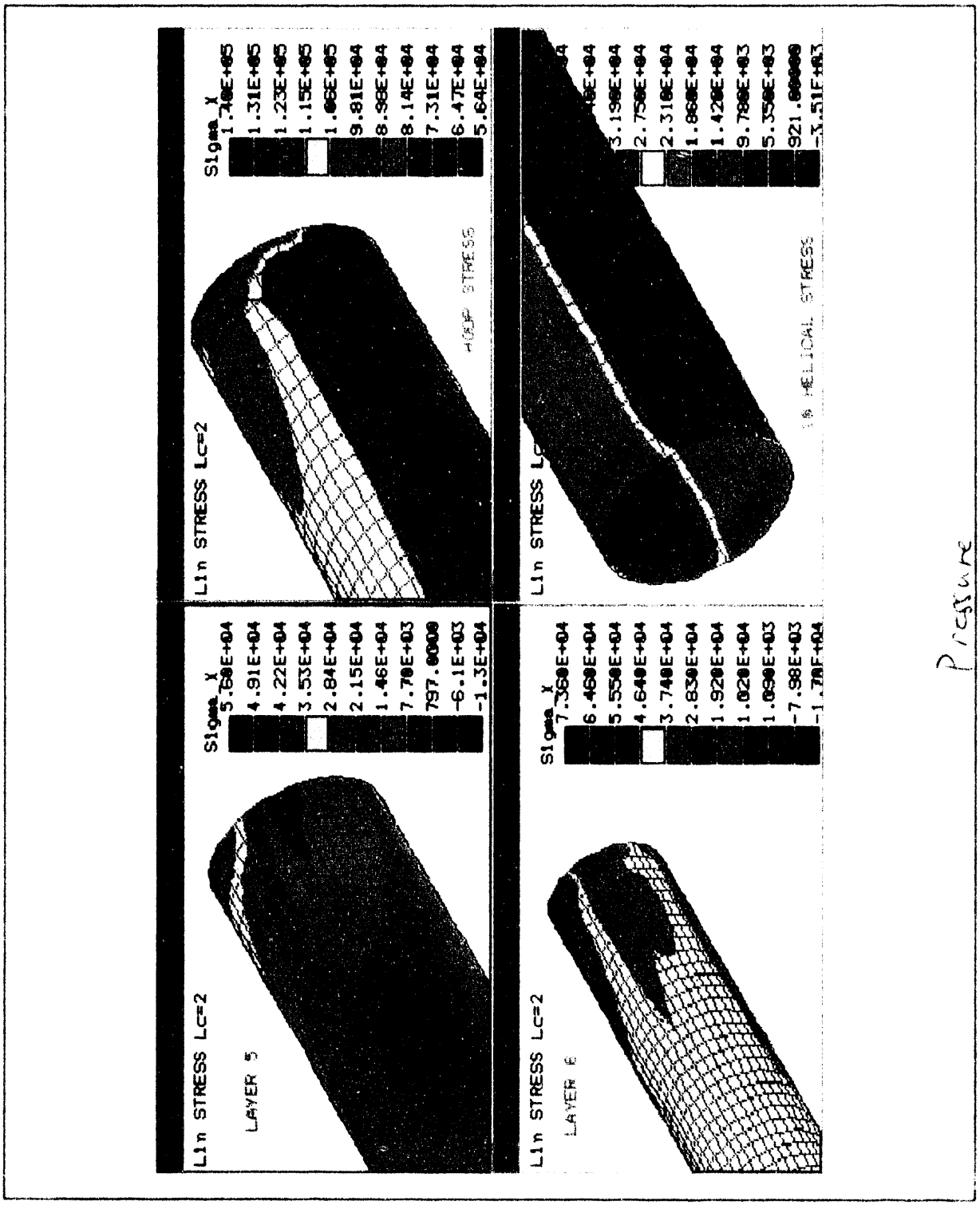
Lin STRESS Lc=2
Sigma X
1.74E+05
1.31E+05
1.23E+05
1.15E+05
1.08E+05
9.81E+04
8.98E+04
8.14E+04
7.31E+04
6.47E+04
5.64E+04
AXIAL STRESS
Lin STRESS Lc=2
Sigma X
5.88E+04
4.91E+04
4.22E+04
3.53E+04
2.84E+04
2.15E+04
1.46E+04
7.70E+03
797.8000
-6.1E+03
-1.3E+04
LAYER 5
Lin STRESS Lc=2
Sigma X
7.36E+04
6.46E+04
5.55E+04
4.64E+04
3.74E+04
2.83E+04
1.92E+04
1.02E+04
1.09E+03
-7.98E+03
-1.78E+04
LAYER 8
Lin STRESS Lc=2
Sigma X
3.19E+04
2.75E+04
2.31E+04
1.86E+04
1.42E+04
9.78E+03
5.35E+03
921.8000
-3.51E+03
RADIAL STRESS

Pressure

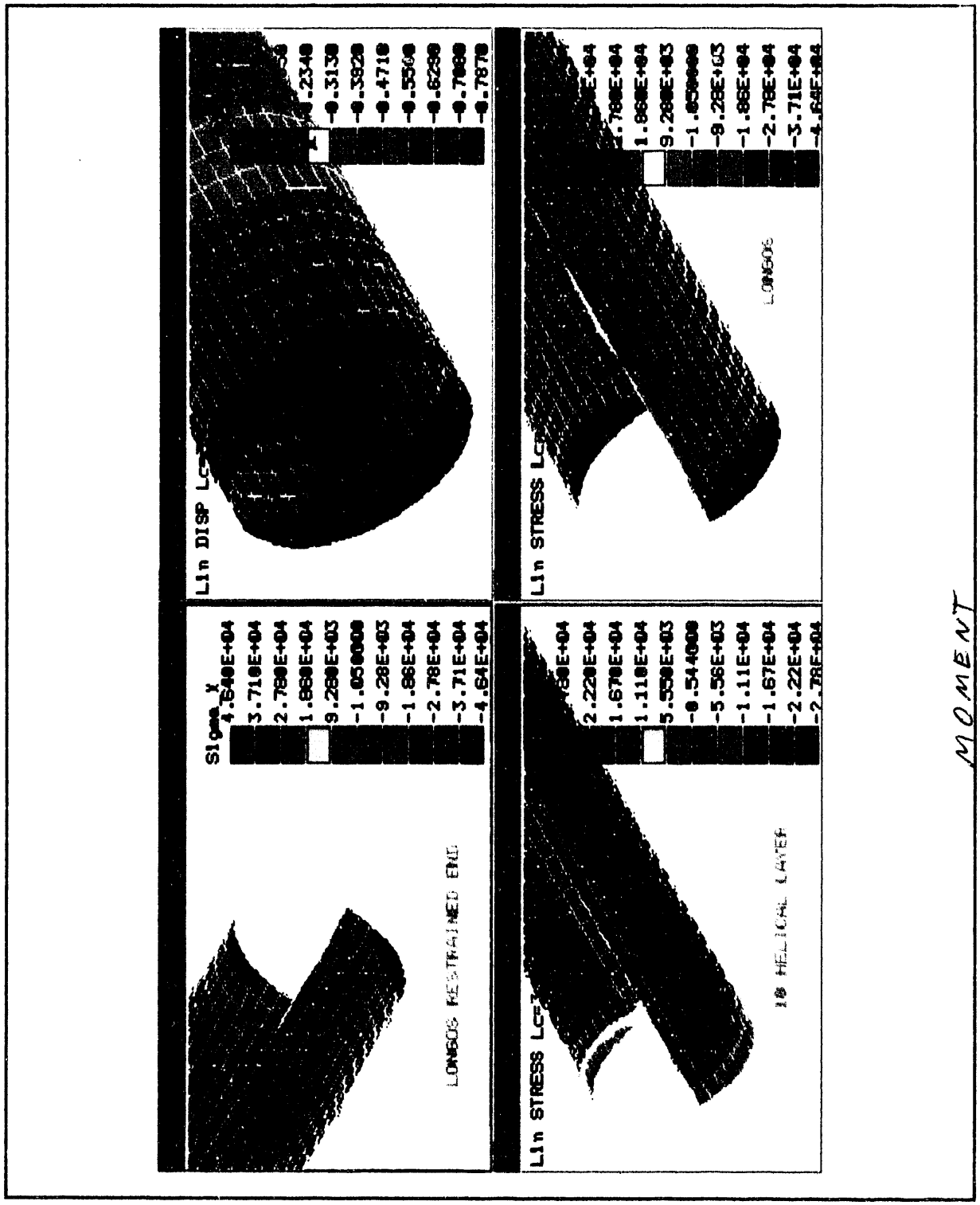
L1n DISP
-0.3138
-0.3923
-0.4710
-0.5500
-0.6280
-0.7080
-0.7870
Sigma X
4.640E+04
3.710E+04
2.780E+04
1.850E+04
9.280E+03
-1.050000
-9.28E+03
-1.86E+04
-2.78E+04
-3.71E+04
-4.64E+04
L1n STRESS
L1n STRESS
1.850E+04
9.280E+03
-9.28E+03
-1.86E+04
-2.78E+04
-3.71E+04
-4.64E+04
2.220E+04
1.670E+04
1.110E+04
5.550E+03
-5.56E+03
-1.11E+04
-1.67E+04
-2.22E+04
-2.78E+04
MOMENT

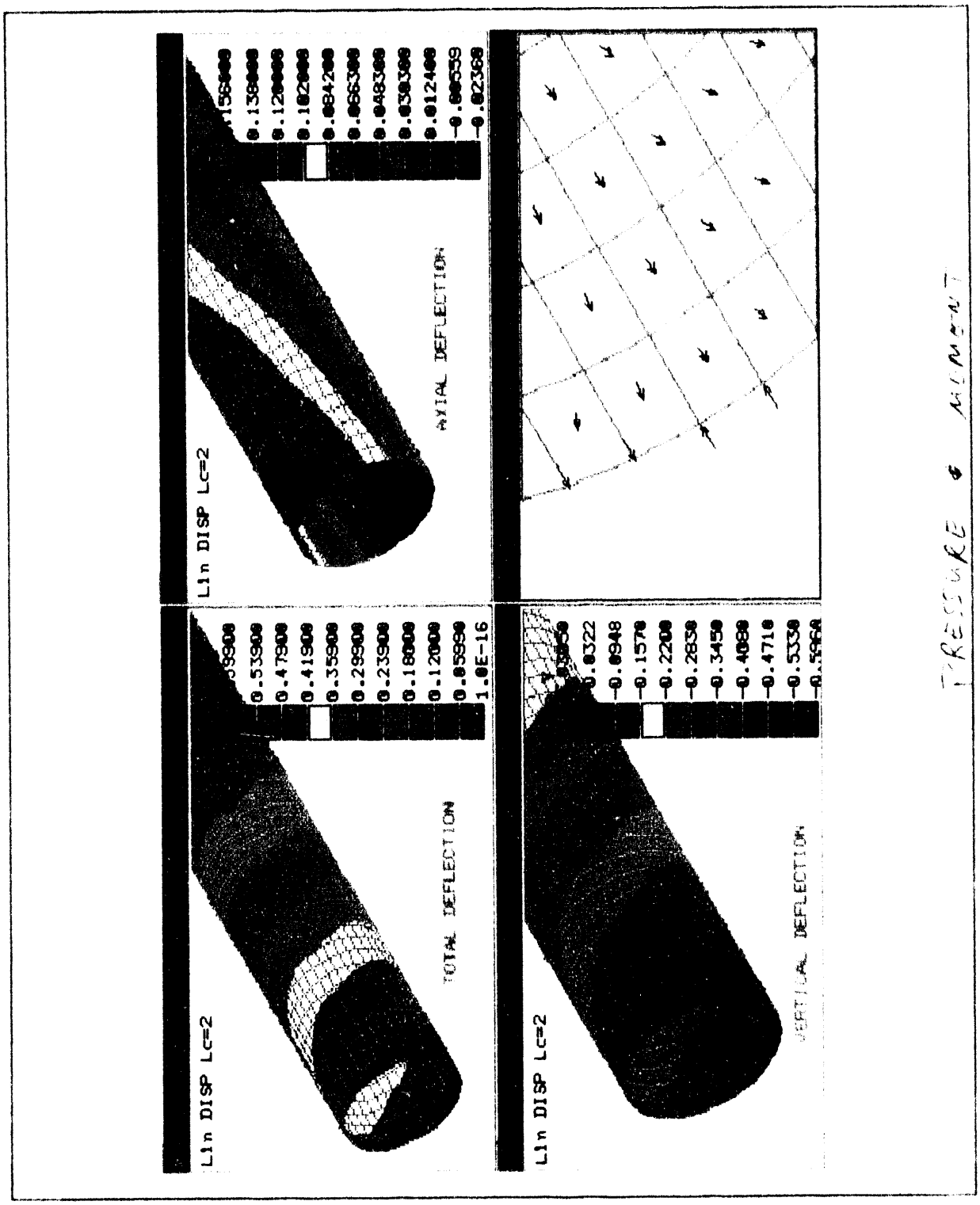
L1n DISP Lc=2
AXIAL DEFLECTION
0.1388
0.1202
0.1016
0.08424
0.06686
0.04948
0.03209
0.01471
-0.00268
-0.02006
PRESSURE & MOMENT
L1n DISP Lc=2
TOTAL DEFLECTION
0.5390
0.4790
0.4190
0.3590
0.2990
0.2390
0.1790
0.1200
0.05990
1.0E-16
L1n DISP Lc=2
VERTICAL DEFLECTION
-0.0322
-0.0948
-0.1574
-0.2200
-0.2826
-0.3452
-0.4078
-0.4704
-0.5330
-0.5956

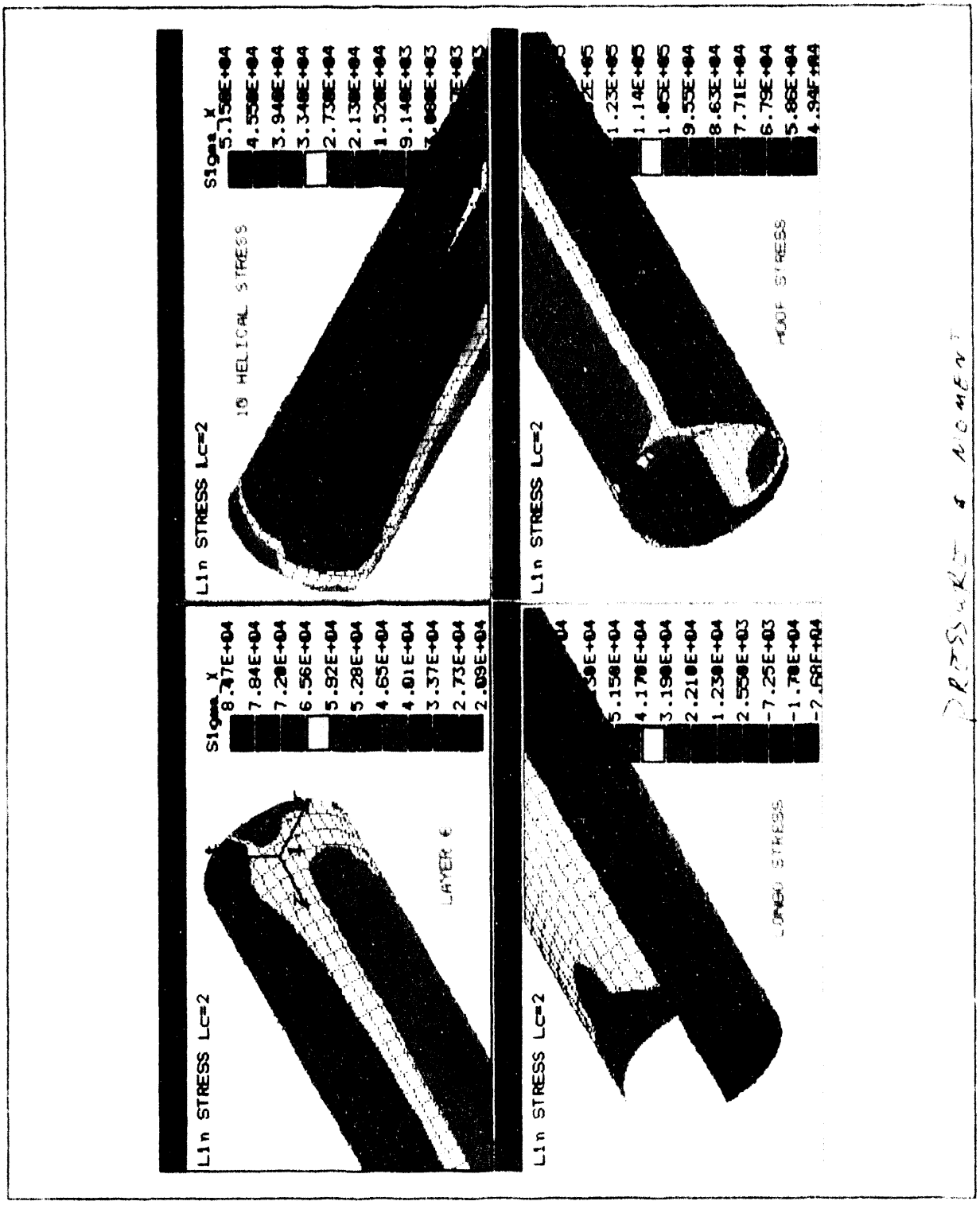
Sigma X
5.15E+04
4.55E+04
3.94E+04
3.34E+04
2.73E+04
2.13E+04
1.52E+04
9.14E+03
L1n STRESS Lc=2
10 HELICAL STRESS
Sigma X
8.47E+04
7.84E+04
7.20E+04
6.56E+04
5.92E+04
5.28E+04
4.65E+04
4.01E+04
3.37E+04
2.73E+04
L1n STRESS Lc=2
LAYER 6
L1n STRESS Lc=2
L1n STRESS Lc=2

DATE
FILMED
5/17/94
END